AADE-25-NTCE-009

Predicting Effects of LCM Particles on Rheology of Spacers and Cements – Part II

Afshin Ahmady, Ronnie G. Morgan, Paul Jones and William Pearl, Halliburton Energy Services, Inc.

Abstract

In Part I of this study, Ahmady et al. (2024) developed a mathematical model for predicting the effects of LCMs (loss circulation materials and other particle systems) on the rheology of spacers and cement slurries (suspension fluids). The uniqueness of the Part I study was that the model predicted a multiplier for each viscometer RPM vs Torque reading from measuring rheology of the suspension fluids without LCMs present. This provided improved convenience and accuracy by allowing conventional viscometers to be used, since no LCMs were present which often presents "clearance challenges" with conventional bob and sleeve viscometers. This approach allowed for efficient fitting of RPM versus dial readings to the desired viscometric model. Part II expands this research to higher LCM concentrations, increasing the volume fractions from 0.13 to 0.18. It also employs advanced rheological measuring devices, including modified and 3D-printed bob and sleeves for viscometers, to improve accuracy and capture complex non-Newtonian behaviors like shear-thinning and yielding effects.

A broader range of LCM materials, shapes, and sizes were tested under diverse fluid conditions to enhance the model's predictive capabilities. For example, new experiments with the R1/B5 bob configuration addressed centrifugal stratification, and the results validated the model's applicability to large particle sizes and higher concentrations. These advancements provide critical insights for optimizing spacer and cement performance in loss-prone drilling environments. The improved model achieved over 94% of predictions within ±20% for a wide range of scenarios.

Introduction

Loss circulation materials (LCMs) are widely used to mitigate fluid losses during drilling and cementing operations. Accurate rheological data for LCM-laden fluids is critical for designing practical effective spacers and cement slurries for a wide range of cement jobs. However, traditional bob and sleeve viscometers often fail to measure rheology accurately due to particle jamming or centrifugal stratification. Part I of this study (Ahmady et al., 2024) addressed these challenges by introducing a modular multiplier-based model to predict the effects of LCMs on rheology, given rheology data from the clean suspension fluid (fluid without LCMs).

This paper focuses on extending the initial model to higher LCM concentrations and incorporating additional factors such as advanced viscometric tools and fluid-property interactions. The work includes new experimental data and enhanced modeling techniques, expanding the understanding of LCM behavior in spacer and cement systems.

Tonmukayakul et al. (2006) developed and tested a viscometer for measuring the rheological properties and settling behavior of fracturing type solutions (CMHPG) and cross-linked HPG solutions for a wide range of volume concentrations, ranging from 0.083 to 0.52. Their work confirmed the findings of Ouchiyama and Tanaka (1980) about a critical volume concentration at which particle-to-particle collisions begin to affect rheology. Ouchivama and Tanaka (1980) estimated that for spheres of the same size, this critical volume concentration is 0.127.

Einstein's (1906) original work to predict the volumetric effects of solid particles on the viscosity of fluids was for concentrations below where particle-to-particle collision occurs. Einstein's legendary equation has been widely used for decades as follows:

$$\eta_p = \eta_0\ (1 + K f_v) \qquad [1]$$

where: η_p is viscosity of the fluid with the solid particles; η_0 is viscosity of the fluid without solid particles, i.e., the clean fluid; f_v is the volume fraction of solid particles; and K is a coefficient that Einstein reported to be 2.5 for low concentrations of spheres.

Maron and Pierce (1956) developed the following model for volumetric concentrations from very low to near particle packing:

$$\eta_p = \eta_0 \ (1 - f_v/f_{vm})^{-2} \quad [2]$$

where: f_{vm} is the maximum packing concentration.

The classic work by Krieger and Dougherty (1959) is best summarized by their model as follows:

$$\eta_r = (1 - f_v/f_{vm})^{-[\eta]f_{vm}} \quad [3]$$

where: $\eta_r = \eta_p/\eta_0$ the relative viscosity and [η] is the intrinsic viscosity.

Recent work by Vergote et al. (2023) quantified the effects of particle morphology and concentrations of slag suspensions for shear rate ranges of 2.5 to 24.5 1/sec and volume concentrations of 0.01 to 0.16.

Thus, this Part II study was primarily aimed at extending the model developed by Ahmady et al. (2024) to the upper end of volume concentrations of LCMs in spacers and cement slurries, being 0.18.

Methods

Experimental Setup

To validate the extended model, a series of experiments were conducted using two types of spacers and two types of cement slurries. The experiments were conducted using both LCM packages and individuals with diverse properties. Table 1 summarizes the combinations of LCM properties and fluid conditions used in the experiments.

Table 1. Summary of Experimental Combinations

Fluid types: Two spacers and two cement slurries
Number of LCM types: 9
Number of LCM combinations: 3
LCM generalized shape: spheres; ellipsoids; flakes, fibers
LCM material texture: very hard; hard; stiff rubber; flexible rubber/plastic
Specific gravity of LCMs: 1.07 to 2.68
Shape factor of LCMs: 0.065 to 0.95
Particle sizes of LCMs (D50): 0.4 to 2.4 mm
Range of all particle sizes: 0.1 to 9.5 mm
Range of aspect ratios: 1 to 75
Volume fraction of LCMs: 0.0021 to 0.18
Yield stress of clean fluids: 0.43 to 7.0 Pa
Shear thinning index of clean fluids: 0.31 to 1.0

Testing included configurations with R1/B1 and R1/B5 bob and sleeve conventional viscometers.

Bi	OD	Ri	ID	Clearance
B1	34.49	R1	36.83	1.17
B2	24.55	R1	36.83	6.14
B5	**31.97**	**R1**	**36.83**	**2.43**

Table 2. Dimensions of bob and sleeve for R1/B1, R1/B2 and R1/B5 configurations, units are in mm.

Additionally, a 3D-printed FYSA viscometer bob and sleeve was deployed to accommodate larger LCM sizes and mitigate particle stratification. The 3D-printed FYSA device was based on a patent by Johnson and Morgan (2005) which replaces the conventional smooth surfaced bob and sleeve with intermeshing fins located on the bob and sleeve. The purpose of the intermeshing fins is to keep particles suspended in a 3D space while RPM vs Torque readings can be made on fluids that are suspending a wide range of particles, such as LCMs.

Figure 1 is a photo of the FYSA viscometer with metal intermeshing fins. The intermeshing fins provide for constant clearances that enhance the accuracy of the mixer type viscometer. Figure 2 illustrates how the original FYSA device was modified to accommodate larger LCM particles by increasing the clearance between the intermeshing fins.

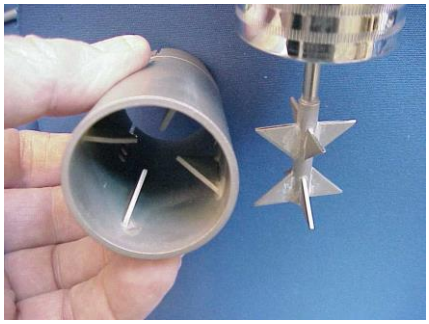

Figure 1. Photo of actual viscometer with intermeshing teeth that was adapted to a conventional bob and sleeve viscometer.

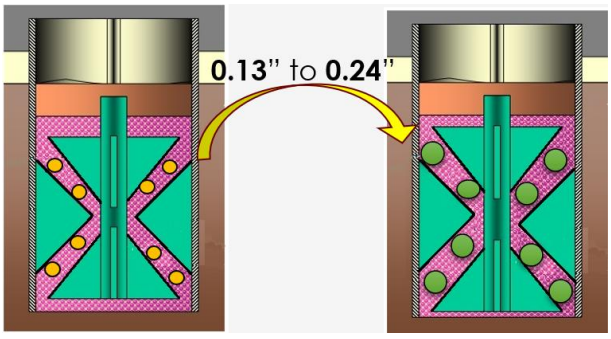

Figure 2. Comparison of standard FYSA mixing viscometer with fin-to-fin clearance of 0.13 inches to the 3D printed FYSA

with enlarged clearance of 0.24 inches to accommodate larger LCM particles.

Figure 3 is an illustration of the 3D Printed FYSA with the enlarged fin-to-fin clearance.

Figure 3. 3D printed FYSA with ceramic materials.

Model Development

Equation [4] was the original model from Ahmady et al. (2024)

$$\frac{DR_{rpm,lcm}}{DR_{rpm}} = [Conc.][Shape][Size][Shear\ Thinning].. \\ ....[Yield\ Stress][Density\ Ratio] \quad [4]$$

Where: $DR_{rpm,lcm}$ = viscometer dial reading at given RPM and concentration of lcm; DR_{rpm} = viscometer dial reading at same rpm for clean fluid without LCM; [Conc.] = multiplier for volume concentration effects; [Shape] = multiplier for particle shape effects; [Size] = multiplier for size effects; [Shear Thinning] = multiplier for shear thinning effects of clean carrier fluid; [Yield Stress] = multiplier for effects of yield point of clean carrier fluid; and [Density Ratio] = multiplier for effects of differences in particle specific gravity and specific gravity of the clean carrier fluid.

Each of the "modular multiplier functions" were selected such that each meets the boundary condition of not being zero. Additionally, each "modular multiplier function" is dimensionless except for the [Size] module which has the units of mm. These "modular multiplier functions" are defined as follows:

$$[\text{Conc}] = K_{oo} + K_{fv}(f_v^{\alpha_{fv}}) \quad [5]$$

$$[\text{Shape}] = SF^{\alpha_{sf}} \quad [6]$$

$$[\text{Size}] = (1 + D_{50})^{\alpha_{d50}} \quad [7]$$

$$[\text{Shear Thinning}] = \left(\frac{3n}{2n+1}\right)^{\alpha_n} \quad [8]$$

$$[\text{Yield Stress}] = \left(1 + \frac{\tau_o}{K_2\ DR_{rpm}}\right)^{\alpha_{ss}} \quad [9]$$

$$[\text{Density Ratio}] = (1 + NDR)^{\alpha_{NDR}} \quad [10]$$

$$\text{NDR} = absolute\ v.\left(\frac{SG_f - SG_{lcm}}{SG_f}\right) \quad [11]$$

The original model was expanded to include higher LCM concentrations and revised multiplier functions to account for shear-thinning and yield stress effects.

The key modular functions were updated as follows:

- [Conc]: Revised to include volume fractions up to 0.18
- [Size]: Enhanced for larger particle sizes
- [Shape]: Refined for complex geometries like fibers and flakes
- [Density Ratio]: Improved for heterogeneous LCM mixtures

Equations [5] has been modified to [5.1], and Equations [6] through [10] were adjusted based on experimental data, resulting in improved accuracy and reduced prediction errors.

$$[\text{Conc}] = \left(K_{oo} + K_{1,fv}.f_v + K_{2,fv} \cdot f_v^{\alpha_{2,fv}} + K_{3,fv} \cdot f_v^{\alpha_{3,fv}}\right) \quad [5.1]$$

The model was validated against measured viscometer readings, showing high reliability across various fluid and particle conditions given in Table 1.

Results and Discussion
Model Performance

The improved model demonstrated robust performance across all tested scenarios. The key findings include:

- **Accuracy:** About 94% of predictions fell within ±20% error, and 87% were within ±15%.
- **Error Reduction:** The average absolute error of original model decreased from 8.8% to 7.902%.
- **Higher Concentrations:** The model accurately captured rheological behaviors at volume fractions up to 0.18, confirming its applicability to challenging operational conditions.

Table 3 is an illustration of how to apply the above-revised Part II model to RPM vs. Dial readings taken for a clean spacer fluid without LCMs. In Table 3, medium-sized LCM particles were added to the spacer, and the composite fluid

with LCM was measured with the FYSA bob and sleeve. The measured rheology data were compared with the respective predicted dial readings.

RPM	Dial Reading, without LCM	Dial Reading, with LCM, observed	Dial Reading, with LCM, Predicted
3	5.5	**10.0**	**9.12**
6	6.5	**11.0**	**10.70**
100	10	**17.5**	**16.22**
200	13	**21.0**	**20.94**
300	17	**25.0**	**27.21**

Table 3. Example 1: FYSA Dial Reading Data (Spacer + Medium Size LCM Particle)

Table 4 is an example of the Part II model's accuracy in developing reliable viscometer parameters. In this case, the Generalized Herschel Bulkley model (Becker, 2003) was fit to the data collected for a spacer with medium-sized LCM particles.

Type of Rheology Test	Mu,oo (cP)	Tau,o (lbf/100ft^2)	m	n
Rheology data for clean	13.57	7.53	1	0.401
Rheology incl. LCM - Actual	**34.58**	**14.7**	**1**	**0.401**
Rheology incl. LCM -Model	**30.24**	**15.6**	**1**	**0.401**

Table 4. Example 1: Generalized Herschel Bulkley Rheology Data (Spacer + Medium Size LCM Particle)

Rheological Insights

Shear-thinning and yield stress effects were pronounced at higher concentrations. The use of the R1/B5 and modified FYSA viscometers minimized errors caused by centrifugal stratification, enabling reliable measurements for large particles.

Figure 4 illustrates the correlation between observed and predicted viscometer readings, highlighting the model's predictive capabilities.

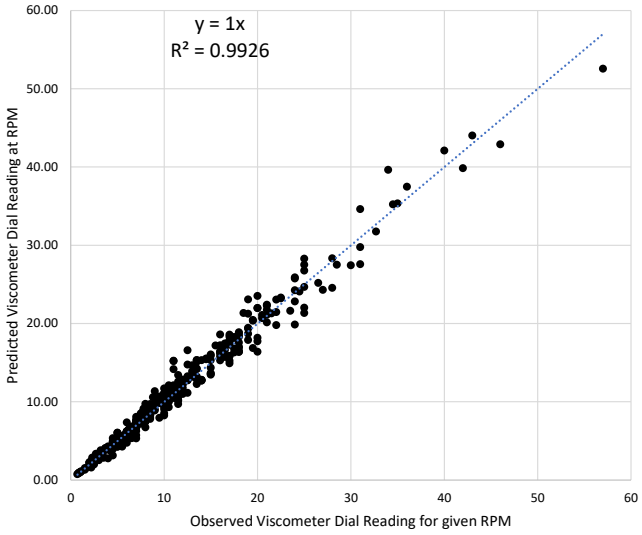

Figure 4. Observed dial readings vs predicted dial readings.

The best fit values for the revised PART II model from the master fit in Figure 4 are:

K_{oo} = 0.98
$K_{1,fv}$ = 2.839
$K_{2,fv}$ = 5.199
$K_{3,fv}$ = 1.00317
$\alpha_{2,fv}$ = 2.066
$\alpha_{3,fv}$ = 5.994
α_{n} = 0.195
α_{sf} = - 0.05
α_{NDR} = 0.313
α_{ss} = 0.043
α_{d50} = 0.084

Conclusions

The true value of this work is that viscometer testing only needs to be performed for clean (without LCMs present) spacers and fluids. Then, the model presented here can be applied to transform the clean RPM vs Dial data to predict viscometric parameters for use in design software. This study also enhances the understanding of LCM rheology by expanding the model to higher concentrations and broader particle properties. The improved model provides a practical tool for optimizing spacer and cement performance in loss-prone drilling environments. Future work will focus on field validation and integrating the model into the cementing hydraulic software for real-time applications.

Acknowledgments

The authors thank Halliburton Energy Services, Inc., for their support and resources in conducting this research. Special thanks to the laboratory team for their assistance in experimental setup and data collection.

Nomenclature

D_{50} = Mass average diameter of particles
$DR_{rpm,lcm}$ = Viscometer dial reading at given RPM and concentration of lcm
DR_{rpm} = Viscometer dial reading at given RPM for clean fluid without LCM
f_v = Volume fraction of particles
f_{vm} = Maximum packing volume fraction
K = Dimensionless coefficient in Eq. [1] and [2]
$K1$ = Coefficient for computing shear rate of viscometer
$K2$ = Coefficient for computing shear stress of viscometer
K_{oo} = Dimensionless coefficient in Eq. [5], [Conc.]
K_{fv} = Dimensionless coefficient in Eq. [5], [Conc.]
$K_{1,fv}$ = Dimensionless coefficient in Eq. [5.1], [Conc.]
$K_{2,fv}$ = Dimensionless coefficient in Eq. [5.1], [Conc.]
$K_{3,fv}$ = Dimensionless coefficient in Eq. [5], [Conc.]
n = Shear thinning index of Generalized Herschel-Bulkley fluid
NDR = Normalized Density Ratio in Eq. [10, 11]
SF = Dimensionless shape factor in Eq. [6]
SG_f = Specific gravity of suspending fluid
SG_{lcm} = Specific gravity of LCM particle
α_{d50} = Exponent in Eq.[9], D_{50} must be in units of mm
α_{fv} = Dimensionless exponent in Eq. [5]
$\alpha_{2,fv}$ = Dimensionless exponent in Eq. [5.1]
$\alpha_{3,fv}$ = Dimensionless exponent in Eq. [5.1]
α_n = Dimensionless exponent in Eq. [8]
α_{sf} = Dimensionless exponent in Eq. [6]
α_{SG} = Dimensionless exponent in Eq. [11]
α_{ss} = Dimensionless exponent in Eq. [9]
η_0 = Apparent viscosity of suspending fluid without LCM
η_p = Apparent viscosity of suspending fluid with LCM
$\eta_r = \eta_p/\eta_0$
τ_o = Yield point of suspending fluid without LCM

References

1. Ahmady, A., Morgan, R.G., Jones, P. and Pearl, W. 2024. "Influence of Loss Circulation Materials on Rheology of Spacers and Cements." AADE-24-FTCE-005, AADE Fluids Technical Conference and Exhibition, Marriott Marquis, Houston, Texas, April 16-17, 2024.
2. Tonmukayakul, N., Morgan, R.G., Morgan, R.L. and Morris, J.F. 2006. "A Device to Measure Flow Behavior of Settling Particle Slurries." Transactions of the Nordic Rheological Society, Vol. 14, 2006.
3. Ouchiyama, N. and Tanaka, T. 1980. "Estimation of the Average Number of Contacts between Randomly Mixed Solid Particles." American Chemical Society, November 1, 1980.
4. Einstein, A. 1906. Ann. Phys. iv, 19, 289 (1906).
5. Maron, S.H. and Pierce, P.E. 1956. "Application of Ree-Eyring Generalized Flow Theory to Suspensions of Spherical Particles." Journal of Colloid Science, Volume 11, Issue 1, February 1956, pages 80-95.
6. Krieger, I.M. and Dougherty, T.J. 1959. "A mechanism for non-Newtonian flow of suspensions of rigid spheres." Transactions of the Society of Rheology 3: 137-152.
7. Vergote, O., Bellemans, I., den Bulck, A.V., Shevchenko, M., Starykh, R., Jak, E., Verbeken, K. 2023. "Viscosity Experiments of Slag-Spinel Suspensions: The Effect of Volume Fraction, Particle Size and Shear Rate. Journal of Rheology, 67, 1159-1174 (2023).
8. Johnson. J.W. and Morgan, R.G. 2005. "Yield Point Adaptation for Rotating Viscometers." US patent # 6,874,353 B2. April 5, 2005.
9. Becker, T.E., Morgan, R.G., Chin, W.C., and Griffith, J.E. 2003. "Improved Rheology Model and Hydraulics Analysis for Tomorrow's Wellbore Fluid Applications." SPE 82415, SPE Production and Operations Symposium, Oklahoma City, OK, March 22-25, 2003.